Chapter 7

Quaternary Faulting on the Solitario Canyon Fault

By Alan R. Ramelli,[1] John A. Oswald, Giovanni Vadurro, Christopher M. Menges, and James B. Paces

Contents

Abstract

Quaternary activity along the Solitario Canyon Fault, one of the principal north-striking, block-bounding normal faults close to the proposed repository site for the storage of high-level radioactive wastes at Yucca Mountain, was studied in 11 trenches and one natural exposure that span the fault in various places. Detailed mapping of the geologic relations exposed at these sites shows a sequence of surficial deposits, ranging in age from early Pleistocene to Holocene, that can be correlated with the general Quaternary stratigraphic framework established for the area, and which have been involved to varying degrees in surface-rupturing paleoearthquakes on the Solitario Canyon Fault.

In chronological order from youngest to oldest, interpreted faulting (and fracturing) events on the Solitario Canyon Fault include (1) two episodes of fracturing that postdate the youngest recognizable faulting event but did not involve discernible structural displacement; (2) the most recent faulting event (Z), dated at 40–20 ka, with offsets of 10 to 20 cm; (3) a penultimate faulting event (Y), the largest and best documented Quaternary faulting event along the Solitario Canyon Fault, which is characterized by fault fissures as much as 70 cm wide filled with basaltic ash correlated with the eruption of the nearby Lathrop Wells volcanic center at 77±6 ka and with cumulative dip-slip displacements of as much as 1.3 m; and (4) two older mid-Quaternary to late Quaternary faulting events (W, X), bracketed between 250–150 and 118±6 ka, which are evidenced by silt- and gravel-filled fault fissures that indicate dip-slip offsets of 20 to 60 cm.

Stratigraphic and structural relations within the exposed surficial deposits indicate little, if any, activity along the Solitario Canyon Fault for a period of several hundred thousand years before event W, although evidence was observed of one or more surface-rupturing paleoearthquakes before this hiatus, likely during early Quaternary time.

The occurrence of as many as four faulting events within a time period of about 200 k.y. indicates an average recurrence interval of about 50 k.y. during mid-Quaternary to late Quaternary time. A recurrence interval of about 35 k.y. is considered to be a minimum for the most recent and penultimate faulting events. The average slip rate for mid-Quaternary to late Quaternary fault activity appears to range from 0.01 to 0.02 mm/yr, on the basis of an average of 2.0 m of slip over 200 k.y. and 1.2 m of slip over 75 k.y.

Introduction

The Solitario Canyon Fault (fig. 2), which extends along the steep west flank of Yucca Mountain (fig. 1), is a major block-bounding fault that forms the west boundary of the

[1]Nevada Bureau of Mines and Geology, Reno.

Table 20. Summary of stratigraphic relations and correlations in trenches across the Solitario Canyon Fault in the Yucca Mountain area, southwestern Nevada.

[See figures 1 and 2 for locations. See table 3 for soil-horizon terminology. Units on east side of Yucca Mountain after Wesling and others (1992); units in Crater Flat from Peterson and others (1995). Do., ditto]

Stratigraphic unit	Trench	Unit	Soil	Correlative unit	
				East side of Yucca Mountain	Crater Flat
Eolian silt/ colluvium.	SCF–T3 SCF–T4 SCF–T2	11–12 9–10 10–11	Av	Qa5	Little Cones.
Eolian silt/ gravel.	T8 SCF–T1	14 20–22	$CaCO_3$ stage I+	Qa5	Do.
Gravelly silt------	T8 SCF–T4 SCF–T2	14 8 8–9	Bw/Bt	Qa4	Late Black Cone.
Gravel ----------	SCF–T1	12–19	Bt/Btk	Qa4	Do.
Stratified gravel.	T8	5–9	Bqkm	Qa3	Early to late Black Cone.
Silty gravel--------	T8	2–4	Bq	Qa3?	Early Black Cone(?).
Gravel ----------	T8 SCF–T1 SCF–T3 SCF–T4 SCF–T2	1 1–8 1–9 1–6 1–7	K	Qa1	Solitario.

Table 21. Numerical ages of deposits exposed in trenches T8, T8A, and SCF–T3 across the Solitario Canyon Fault in the Yucca Mountain area, southwestern Nevada.

[See figures 1 and 2 for locations. Samples: TL– (error limits, ±2σ), thermoluminescence analyses by S.A. Mahan; HD (error limits, ±2σ), U-series analyses by J.B. Paces]

Trench	Sample	Unit and material sampled	Estimated age (ka)
8 (fig. 31)	TL–30	11a, fissure fill----------	36±3
	HD 1070	10, rhizolith in fissure fill----------	27±1, 37±2, 39±1, 40±3, 48±5, 56±3
	HD 1071	11a, carbonate in vein----------	15±4, 15±7, 16±3, 16±3
	HD 1072	Carbonate stringer in fracture----------	114±5, 117±5, 119±6, 124±6
	HD 1465	12, composite soil sample----------	47±9, 66±23
8A	TL–10	Upper part of Av soil horizon----------	11±2
	TL–11	Lower part of Av soil horizon----------	14±2
SCF–T3 (fig. 34)	HD 1726	7, opaline silica in clast rind----------	144±4, 324±7, 880±160, 950±140
	HD 1730	8, opaline silica in Kqm soil horizon---	25±0.1, 28±0.2
	HD 1731	8, opaline silica in clast rind, upper part of Kqm soil horizon----------	170±3, 590±110, 870±150, 900±140, 970±450
	HD 1732	8, opaline silica in Kqm soil horizon---	199±10, 233±4, 245±4, 320±7, 394±69

proposed repository site for the storage of high-level radioactive wastes. Quaternary activity along this fault is well documented and, given its proximity to the repository site, is particularly important for assessing seismic hazards.

Characteristics of the Solitario Canyon Fault were shown on the detailed geologic maps of Day and others (1998a, b). As described in chapter 3, the fault can be traced for distances of at least 18 km (fig. 2). A prominent fault scarp, in places forming the bedrock-alluvium contact at the base of the west slope of Yucca Mountain, marks the fault trace for much of its length.

Quaternary deposits identified during the mapping of trench excavations for this study follow the stratigraphic schemes presented for the Yucca Mountain area in table 2 (see chap. 2); lithologic-unit designations and their correlations are summarized in table 20. Ages assigned to subdivisions of the Quaternary period are shown in figure 3 (chap. 2), and estimated ages of specific samples collected and analyzed during the present study are listed in table 21.

Trench Investigations

A total of 13 exploratory trenches or test pits and one natural-wash exposure have been excavated and (or) cleaned across or near the Solitario Canyon Fault (fig. 2). Seven trenches excavated in 1979–80 included three (T8, T10A, T10B) along the central section of the fault and four (GA1A, GA1B, T13, and an unnamed trench at the head of Solitario Canyon [not shown in fig. 2]) along the northern section. Excavations were also conducted at seven sites (trenches SCF–T1 through SCF–T4, SCF–E1, T8A, and a deepening of trench T8) during the present study. Descriptions and logs of five of these trenches (T8, SCF–T1 through SCF–T4) are included in this chapter, as well as a description of test pit T8A.

Interpretations of stratigraphy and fault relations are complicated by extensive silica and carbonate overprinting of the deposits. Along the Solitario Canyon Fault, as elsewhere in the Yucca Mountain area (figs. 1, 2), carbonate accumulation

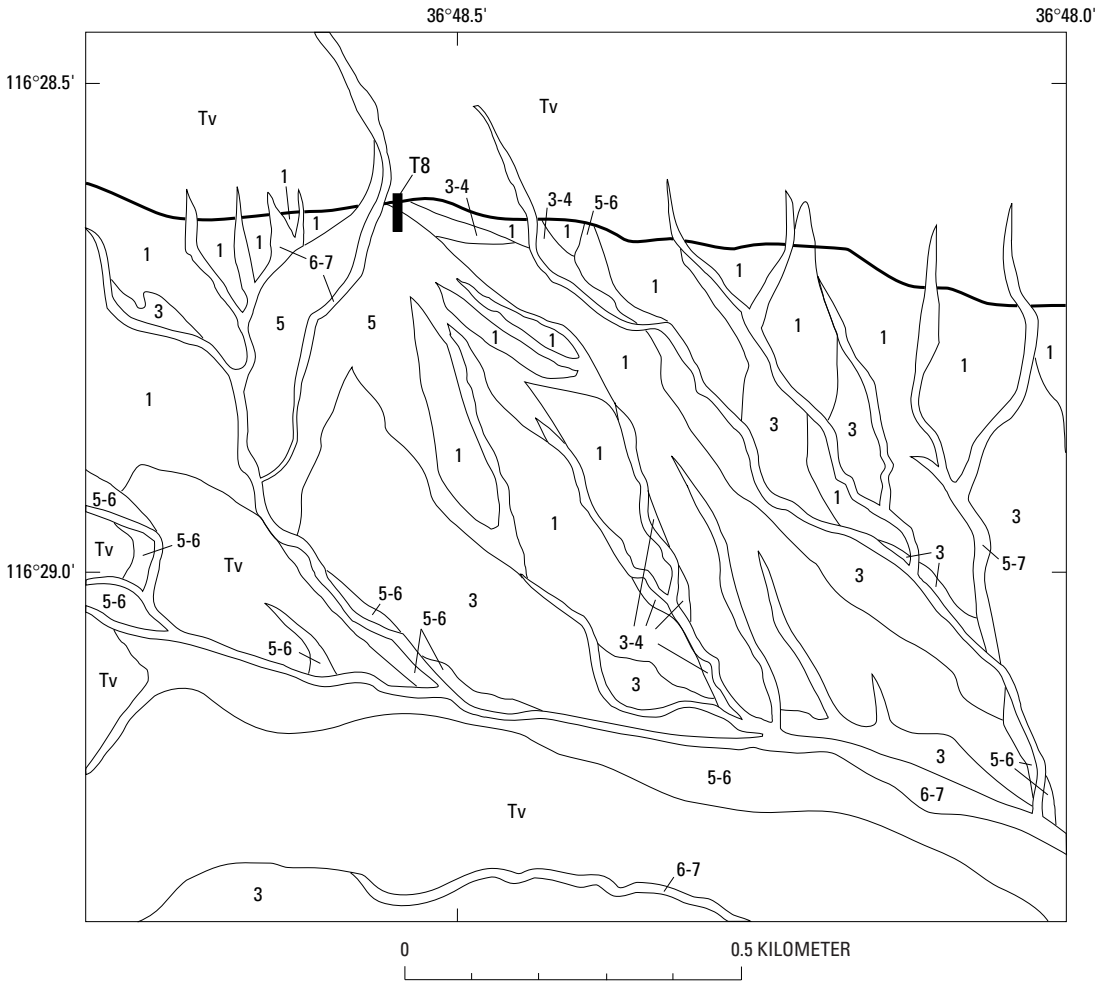

Figure 30. Surficial geologic map of area of trench T8 across the Solitario Canyon Fault in the Yucca Mountain area, southwestern Nevada (figs. 1, 2).

is greatest at and immediately downslope from faults bounding bedrock hillslopes, probably for three reasons: (1) enhanced runoff from the bedrock hillslopes, (2) a pronounced permeability contrast where alluvium is juxtaposed against bedrock, and (3) fractures that allow relatively deep moisture penetration. Morphologic stages of pedogenic carbonate used in this report are based on those of Gile and others (1966), and stages of pedogenic silica on those of Taylor (1986). Soil-horizon nomenclature follows that of Birkeland (1984) and the U.S. Soil Conservation Service. Estimated ages of Quaternary deposits

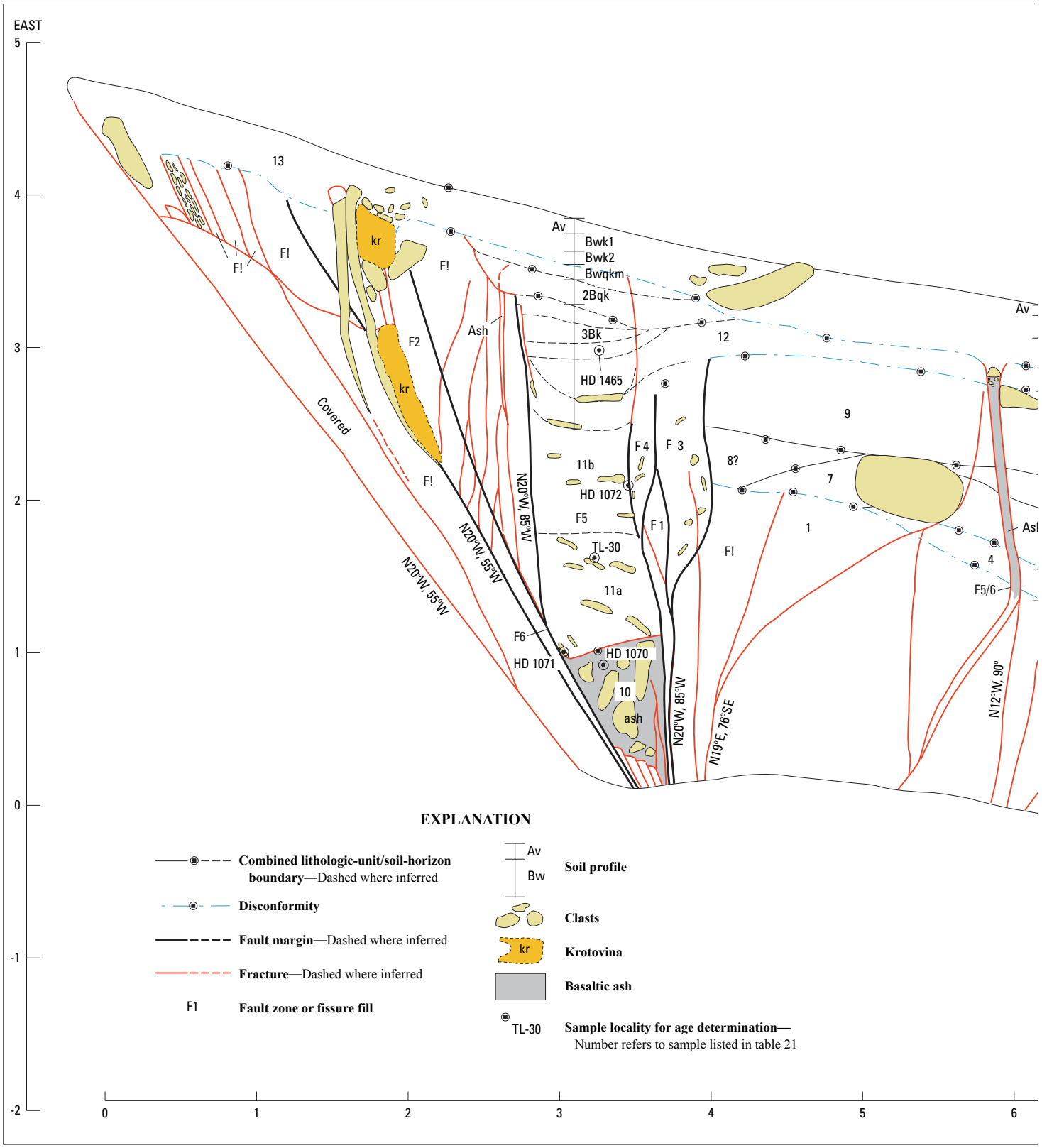

exposed in exploratory trenches and elsewhere are based on U-series and thermoluminescence analyses (table 21), and on comparisons with Quaternary stratigraphic sequences identified in the surrounding region (for example, Wesling and others, 1992; Peterson and others, 1995; see chap. 2; table 2).

Trench T8

Trench T8 (fig. 2), located at the head of an alluvial fan represented by unit Qa5 (fig. 30; table 20), is one of several original trenches excavated for the Yucca Mountain site-char-

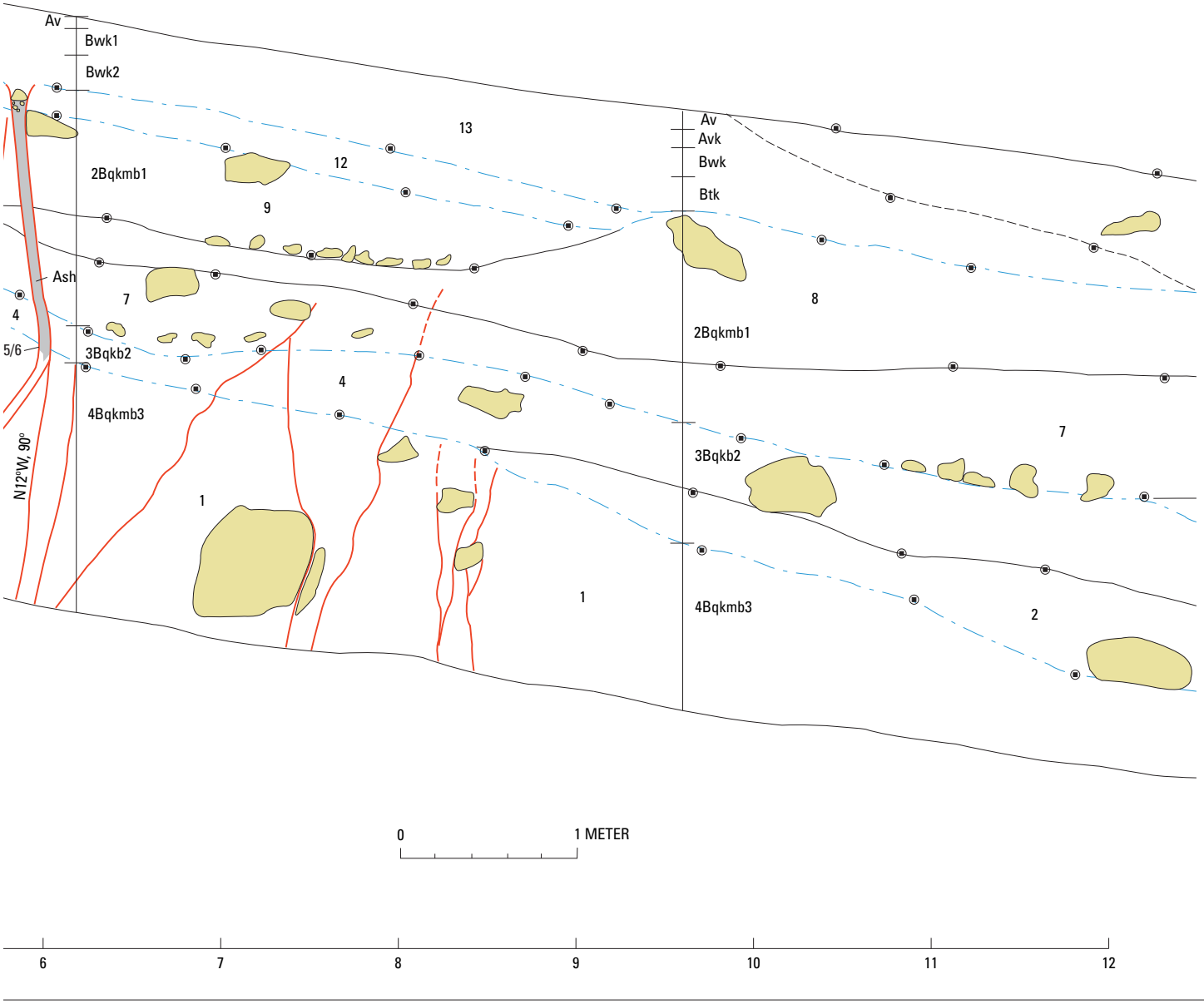

Figure 31. Log of south wall of trench T8 across the Solitario Canyon Fault in the Yucca Mountain area, southwestern Nevada (figs. 1, 2). See table 20 for correlation of map units. See table 3 for explanation of soil horizons; prefixed numbers refer to differentiated soil horizons with increasing depth, and suffixed numbers to further differentiation of properties within an individual soil horizon.

acterization project. The trench was deepened in mid-1993 to provide a better exposure of older faulted deposits, and an adjacent test pit (T8A) was excavated at that time to further assess the recency of faulting. Trench T8 exposes fanglomerate gravel deposits downthrown against welded Miocene tuff (nonlithophysal zone of the crystal-rich member of the Topopah Spring Tuff; Day and others, 1998a). The Quaternary deposits, which are exposed only on the hanging wall, are divided into five distinct age groups, each with distinguishing soil development. Most, if not all, of these age groups are represented in the fairly complex surficial geology of the alluvial fan at this site (figs. 30–32). The tuff lies basically at the ground surface on the footwall and is covered locally by a thin deposit of relatively young eolian silt and colluvium. A small strath terrace is apparently cut into the tuff on the upthrown side of the fault.

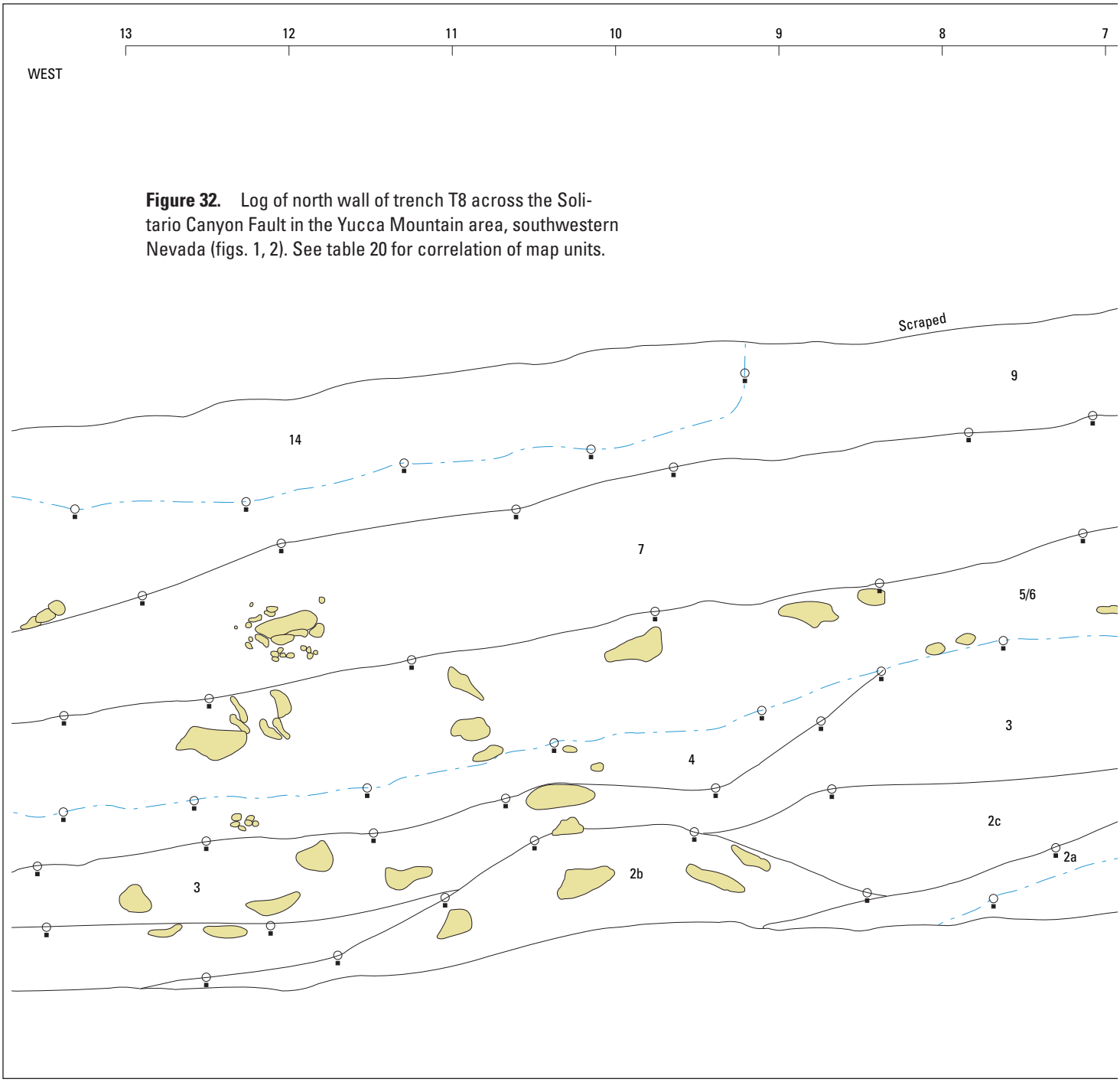

Figure 32. Log of north wall of trench T8 across the Solitario Canyon Fault in the Yucca Mountain area, southwestern Nevada (figs. 1, 2). See table 20 for correlation of map units.

Stratigraphy

The lowermost gravel deposits (unit 1, fig. 30) exposed in trench T8 (fig. 2) consist of bouldery gravel entirely engulfed in silica and carbonate ($CaCO_3$ stage III–V morphology) that have obliterated most of the original sedimentary fabric and contacts. The upper soil horizons associated with this massive petrocalcic horizon have been erosionally stripped. These gravel deposits are best exposed in the south wall of the trench (fig. 31) but are also exposed near the bottom in the north wall (fig. 32). The deposits are widely exposed across the southern and eastern parts of the alluvial fan in which trench T8 is excavated (fig. 30). On the basis of extensive silica and carbonate accumulation and stratigraphic position, unit 1 is dated at middle Pleistocene, possibly early Pleistocene (probably >500 ka) and is correlated with the oldest Quaternary deposits (unit Qa1, table 20) generally present in the Yucca Mountain area (figs. 1, 2).

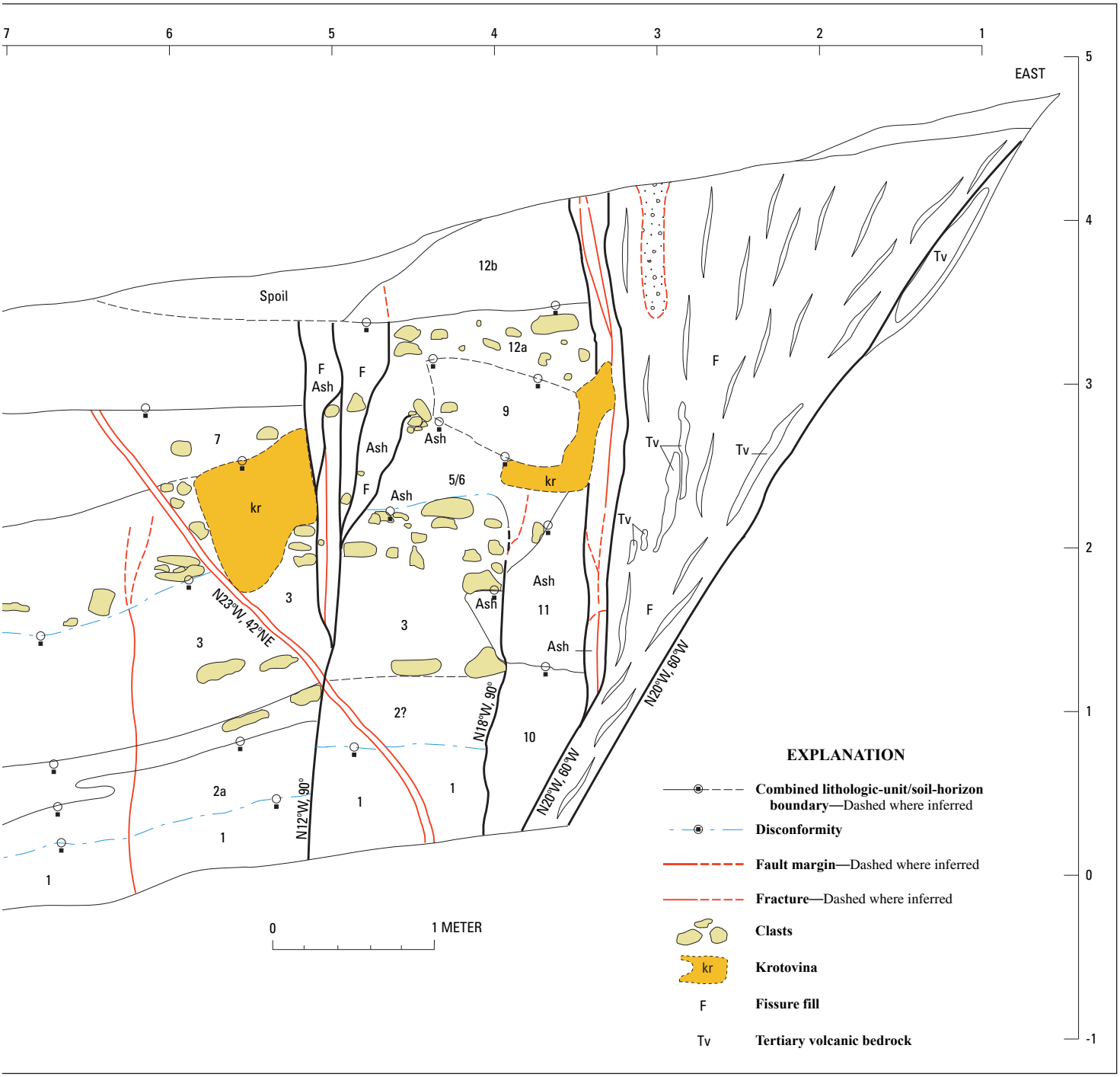

Unit 1 is overlain by gravel deposits (units 2–4, fig. 30) with a distinctive brown noncalcareous silt matrix that is moderately to strongly cemented by silica. The material was deposited in a channel just north of trench T8 (fig. 2), in the vicinity of the current active wash, and the deposits are much thicker in the north wall (fig. 32) than in the south wall (fig. 31). The only constraint on the age of units 2 through 4 is their stratigraphic position; they are likely closer in age to the overlying deposits (believed to be of unit Qa3 age; see chap. 2; fig. 3) and so are probably middle Pleistocene.

A group of moderately well stratified alluvial pebble-and-cobble gravel deposits (units 5–9, fig. 30) represents an episode of alluviation not evident at the other trench sites along the Solitario Canyon Fault. These deposits contain a well-developed petrocalcic horizon ($CaCO_3$ stage III–IV morphology), but silica and carbonate accumulations do not obliterate the sedimentary fabric. The upper soil horizons associated with this petrocalcic horizon were erosionally stripped before younger material was deposited. On the basis of stratigraphic position, carbonate accumulation, and a U-series age on material from an adjacent fracture fill (stas. 3.5–4 m, fig. 31; sample HD 1072; table 21; average age, 118±6 ka) that crosscuts and therefore postdates the deposits, units 5 through 9 are dated at middle to late Pleistocene (150–250 ka) and are tentatively correlated, at least in part, with unit Qa3 (table 20).

Units 10 and 11 were deposited in a 60- to 70-cm-wide subvertical fissure formed during the largest late Quaternary surface-rupturing paleoearthquake. In the south wall of the trench (fig. 31), unit 10 consists of nearly pure basaltic ash and mixed volcanic and carbonate clasts that fill the bottom 1 m of the fissure. The extreme angularity of the ash grains, indicating minimal transport, along with a scarcity of other detrital material (for example, eolian silt), indicates that the ash accumulated in this fissure relatively soon after faulting. In the north wall (fig. 32), unit 10 consists of ash-free pebbly silt apparently deposited just before the ash.

Unit 11, which fills the upper part of this fissure, consists predominantly of silt and fine sand, with minor gravel clasts and reworked basaltic ash; the ash content decreases gradually upward. In the south wall (fig. 31), the lower part of unit 11 (11a) has an inclined sedimentary fabric, likely because this material spilled into the fissure from upslope. The upper part of unit 11 (11b) has a more subhorizontal fabric, probably resulting from a more gradual filling of the fissure from both sides, including material backwasted from the downhill side.

Unit 12 does not have a distinct contact with unit 11 but is distinguished on the basis of position and geometry (it forms a downslope-tapering wedge of material deposited after the fissure was filled). Units 11b and 12 contain carbonate with $CaCO_3$ stage II+ morphology, indicating an age of at least a few tens of thousands of years. A maximum age for units 10 through 12 is provided by the above-mentioned U-series age of 118±6 ka on older fissure carbonate (sample HD 1072, table 21). Minimum limiting ages include (1) U-series ages of 27±1 and 56±3 ka on rhizoliths from within unit 10 (sample HD 1070), (2) a thermoluminescence age of 36±3 ka on material from the middle part of unit 11 (sample TL–30), (3) U-series ages of 47±9 and 66±23 ka on secondary carbonate from within the lower part of unit 12 (sample HD 1465), and (4) an average U-series age of 15.5±4.3 ka on vein carbonate crosscutting the basaltic ash (sample HD 1071). A sample of secondary carbonate from the upper part of unit 12 was dated at 101±4 ka, but this age was discounted because of poor sample quality and inconsistency with other results.

On the basis of geochronologic data, carbonate accumulation, and stratigraphic position, units 10 through 12 are dated at late Pleistocene (40–100 ka). Correlation with the largest eruption at the nearby Lathrop Wells volcanic center (fig. 1) indicates an age of 77±6 ka (Heizler and others, 1999) for unit 10.

A gravelly-silt deposit (unit 13, fig. 31), composed of colluvium, eolian silt, and possibly minor amounts of alluvial gravel, extends across the Solitario Canyon Fault, overlying unit 12, the fault zone, and welded tuff in the footwall. The deposit contains a weak argillic (Bt) horizon, and exhibits soil catena characteristics, wherein soil development increases downslope. Owing to the ongoing input of eolian material, the deposit is time transgressive, as evidenced by the soils and by its interfingering relation with the overlying unit 14. Thermoluminescence ages of 11±2 and 14±2 ka (samples TL–10 and TL–11, respectively, table 21) were obtained for this deposit in test pit T8A (fig. 2), a small excavation across the fault 5 m south of the main trench T8. Unit 13 is dated at late Pleistocene to Holocene and is correlated with units Qa4 and (or) Qa5 (table 20).

The uppermost deposit (unit 14, fig. 32) consists of silty alluvial gravel, about 1 m thick, that is present only downslope from the fault, and so it appears to have no direct relation to faulting. Soil development within this deposit is minimal, consisting of a fairly thin vesicular A (Av) horizon, cambic (Bw) horizon, and $CaCO_3$ stage I–I+ morphology. Unit 14 is dated at latest Pleistocene or Holocene and is correlated with unit Qa5 (table 20).

Structure

Trench T8 (fig. 2) exposes a west-dipping bedrock fault expressed as a 3- to 5-m-wide, flaring-upward zone that separates welded tuff in the footwall from alluvial gravel in the hanging wall. The fault zone is composed largely of laminar or massive silica and carbonate, carbonate-cemented gravel, slivers of tuff, and fissures filled with silt, gravel, and basaltic ash. Of all the trenches on the Solitario Canyon Fault, trench T8 exposes the largest displacements and provides the most complete record of mid-Quaternary to late Quaternary activity. The following discussion outlines evidence of apparent faulting events from youngest to oldest, including two possible fracturing events.

Uncemented, silt-filled fractures are present in the south wall of trench T8 (fig. 31) but not in the north wall (fig. 32). Although the absence of cementation of these fractures indicates a minor Holocene fracturing event, several other origins for such silt-filled openings are possible, including (1) bioturbation, (2) carbonate dissolution, (3) root wedging, (4) downslope mass

Table 22. Estimated displacements associated with middle to late Quaternary faulting events along the Solitario Canyon Fault in the Yucca Mountain area, southwestern Nevada.

[See figures 1 and 2 for locations. n.p., not present]

Event	Date (ka)	Trench (displacement in centimeters)				Comments
		SCF–T4	T8	SCF–T3	SCF–T1	
?	15–5	n.p.	0?	0?	n.p.	Silt-filled openings.
?	25–15	n.p.?	0	n.p.?	n.p.?	Cemented fracture.
Z	30–20	0–10?	10–20	0–10?	?	Minor fissure; fracturs in event Y fissure fill; dragged event Y ash.
Y	80–70	20–40	110–130	60–120	50–120	Largest event; fissures contain basaltic ash.
X	200–120	n.p.?	20–40	?	?	15-cm-wide fissure in trench T8.
W	250–150	15–30	30–60	20–40	?	Second-largest faulting event.

movement, (5) compaction, and (6) shrink/swelling. A 20-cm-wide, silt-filled opening in trench T8 (sta. 2 m, fig. 31) that appears to be an animal burrow does not noticeably displace an older gravel-filled fissure. Animal burrowing concentrated along faults is common in the Yucca Mountain area (figs. 1, 2).

A single silica- and carbonate-cemented fracture in the south wall of trench T8 (sta. 3.5 m, fig. 31) cuts all cemented deposits. This cemented fracture is distinctly older than the silt-filled fractures, yet it cuts deposits capping the more definitive displacements discussed below. The narrow, even width of the fracture indicates a slight extensional opening.

The most recent faulting event (Z, table 22) is indicated by (1) carbonate-filled fractures that cut the ash-filled fissure discussed below, (2) basaltic ash dragged along the fault, and (3) a narrow (10–15 cm wide) silt- and ash-filled fissure exposed in the north wall of the trench. These features indicate vertical displacement of about 10 to 20 cm. A U-series age of 15±4 ka on vein carbonate (sample HD 1071, table 21) from the south wall of the trench (fig. 31) provides a possible minimum date for this event.

The penultimate and, by far, largest faulting event (Y, table 22) is evidenced by a silt- and ash-filled fissure exposed in both walls of trench T8 (figs. 31, 32) and in a bench in the middle of the trench. In the south wall, the bottom 1 m of this fissure (unit 10) is filled with jumbled tuff and carbonate clasts in a matrix of loose, nearly pure basaltic ash. The absence of other detrital material indicates that the ash was emplaced soon after the fissure opened and that faulting and basaltic volcanism were essentially contemporaneous. In the north wall, this fissure is less obvious and lacks the nearly pure ash; the bottom is filled with ash-free pebbly silt similar to material (unit 5/6?) that underlies a tilted block of calcrete (unit 9); these materials apparently collapsed into the fissure before the ash was deposited, probably during the paleoearthquake. The upper fissure fill in the north wall is a mixture of silt, ash, and gravel similar to that in the south wall. The fault slip indicated by this fissure can be estimated from the fault dip (58°) and the extensional opening (consistently 60–70 cm) that splays subvertically from the dipping bedrock fault plane at about 4-m depth. The geometry (fig. 33) indicates dip slip of 1.1 to 1.3 m (0.9–1.1 m of vertical displacement). The moderately well developed soil in the upper part of the fissure fill contains thin silica and carbonate laminae in the uppermost 1 m.

Minimum dates for event Y are provided by U-series ages of 47±9 and 66±23 ka on secondary carbonate from unit 12 (sample HD 1465, table 21), and by a thermoluminescence age of 36±3 ka on material from unit 11 (sample TL–30). An average U-series age of 118±6 ka on fissure carbonate predating the faulting event (sample HD 1072) provides a maximum date. The age (77±6 ka) of the basaltic ash erupted from the nearby Lathrop Wells volcanic center (fig. 1), which is a conspicuous component of the fissure fill that is closely associated with event Y, falls within the range of maximum and minimum dates stated above. Accordingly, event Y is interpreted to have been nearly contemporaneous with that eruption.

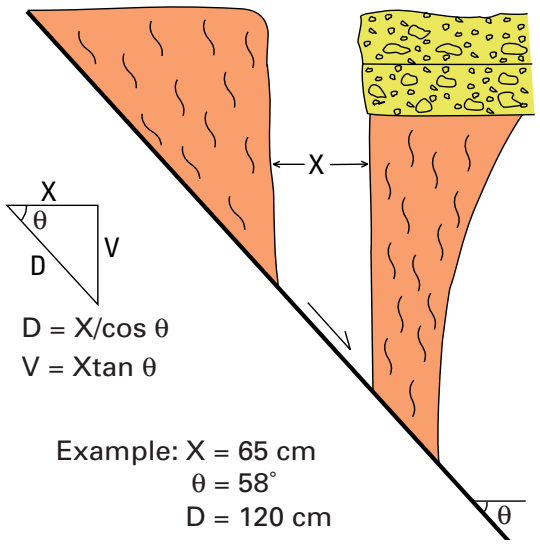

Figure 33. Simple model for estimating fault displacement (D) from genetic constraints imposed by fissure width (X) and fault dip (θ).

Two gravel-filled fissures in the south wall of trench T8 (stas. 3.5–4 m, fig. 31) appears to bound the west side of the ash-filled fissure; both gravel-filled fissures are more highly cemented than, and thus predate, the ash-filled fissure. Furthermore, crosscutting relations and carbonate accumulation indicate that both gravel-filled fissures predate the ash-filled fissure and postdate unit Qa3(?) gravel (units 7–9, fig. 31). The younger and smaller (15 cm wide) gravel-filled fissure represents event X (table 22), whereas the older and larger one (25 cm wide) represents event W (table 20), extending downward into older, massively carbonate cemented fault-zone material. The smaller fissure contains a 2-cm-wide carbonate seam that yielded an average U-series age of 118±6 ka (sample HD 1072, table 21), providing an apparent minimum date for event X. The estimated age (150–250 ka) of the faulted gravel provides an approximate maximum date for event W.

The carbonate-dominated fault zone indicates a faulting event that may predate event W, but defining discrete events within this zone is difficult, owing to carbonate overprinting. A gravel-filled fissure (easternmost fissure at sta. approx 2 m, fig. 31) that reflects one event within this fault zone is highly fractured and crosscut by 1- to 2-cm-thick silica veins but is not obviously displaced by the crosscutting fractures. The secondary silica and carbonate within the fissure indicates a fairly old age; this fissure is the only feature within the older part of the fault zone that retains recognizable sedimentary fabric, and so it may reflect the earliest faulting event preserved in the fault zone.

Test Pit T8A

A small test pit (T8A, fig. 2) was excavated a few meters south of trench T8 to further evaluate Quaternary activity on the Solitario Canyon Fault. The observed stratigraphic and structural relations (not illustrated in this report) are similar to those in the equivalent (upper) part of the south wall of trench T8. Test pit T8A exposes cemented gravel and fault-zone carbonate downthrown against welded tuff. The downthrown units and tuff are overlain by younger mixed colluvium and eolian silt, which is nearly the same deposit as unit 13 in trench T8 but contains a cambic rather than a weak argillic soil. As mentioned previously, thermoluminescence ages of 11±2 and 14±2 ka were determined on two samples (TL–10 and TL–11, respectively, table 21) from this unit in the pit. An irregular, silt-filled opening and multiple narrow silt-filled fractures observed in test pit T8A may indicate Quaternary faulting. Alternatively, these features can also be explained by bioturbation and soil creep.

Trench SCF–T1

Trench SCF–T1 (pl. 8; fig. 2) is located on an active alluvial fan whose surface is dominated by thin (≤1 m thick) gravel deposits of latest Pleistocene or early Holocene age. The trench was excavated across a weak tonal or vegetative lineament apparent on large-scale, low-sun-angle aerial photographs. This lineament and topographic features previously interpreted as small scarps (10–20 cm high) are located on line with the main Quaternary fault scarp along the fault, indicating possible minor Holocene faulting. Trench SCF–T1 was excavated to evaluate this possible faulting and to define the most recent surface rupture on the Solitario Canyon Fault. A smaller test pit was excavated nearby to provide an additional exposure of the uppermost deposits.

Stratigraphy

Trench SCF–T1 (pl. 8) exposes Quaternary fanglomerate gravel that is downthrown against and overlies nonwelded tuff of the lower part of the Tiva Canyon Tuff. The lowermost gravel layers (units 1–4, pl. 8) are present only on the hanging wall of the Solitario Canyon Fault. At the west end of the trench (pl. 8), these deposits are entirely engulfed in silica and carbonate ($CaCO_3$ stage III–V morphology), and much of the original sedimentary fabric is obliterated. On the basis of extensive silica and carbonate accumulation, units 1 through 4 are dated at middle Pleistocene or older (probably >500 ka) and are correlated with the oldest Quaternary deposits (unit Qa1, table 20) generally present in the Yucca Mountain area (figs. 1, 2).

Units 5 through 8 (pl. 8) also are entirely engulfed in carbonate ($CaCO_3$ stage III–IV morphology). These alluvial deposits are distinguished from older lithologic units by an angular unconformity, by differing carbonate accumulation within the vicinity of the fault zone, and by lesser fault deformation. Units 5 through 8 are dated at middle Pleistocene or older (probably >500 ka) and are also correlated with the oldest Quaternary deposits (unit Qa1, table 20) generally present in the Yucca Mountain area (figs. 1, 2).

Units 9 and 10 (figs. 31, 32) are thin, well-cemented ($CaCO_3$ stage III morphology) deposits, possibly scarp colluvium, present on the downthrown side of a minor fault (stas. 22–23.5 m, pl. 8) that cuts units 1 through 8. On the basis of carbonate accumulation and stratigraphic position, units 9 and 10 are loosely correlated with deposits dated at middle to late Pleistocene (probably 50–200 ka).

Moderately well cemented to well-cemented ($CaCO_3$ stage II–III morphology) gravel deposits (units 12–16, pl. 8) overlie bedrock on the upthrown side of the fault. The deposits are present only upslope from the fault (a thin layer of unit 14 is shown toward the east end of pl. 8) but trend obliquely through the trench site and cross the main fault zone that is exposed in the adjacent test pit. Within the pit, the upper part of the deposits (unit 16?) contains a minor amount of reworked basaltic ash. Cementation of units 12 through 16 is markedly less than that of the older deposits. On the basis of stratigraphic position, carbonate accumulation, and the presence of basaltic ash, which is assumed to have been erupted from the Lathrop Wells volcanic center, units 12 through 16 are dated at late Pleistocene and are tentatively correlated with unit Qa4 (table 20).

A minor pebble-gravel deposit (unit 17, pl. 8) along the main fault zone (stas. 10–11 m) may be a small colluvial wedge related to a faulting event of unknown date. The deposit has a $CaCO_3$ stage II morphology, with a single carbonate lamina on top. On the basis of stratigraphic position and carbonate accumulation, unit 17 is tentatively dated at late Pleistocene.

Units 18 and 19 consist of thin, discontinuous silt deposits overlying unit 17 that contain a weakly to moderately cemented argillic (Bt to Btk) soil horizon. This argillic soil must partly be associated with the carbonate accumulation in the underlying gravel deposit, but the silt layers extend with uniform thickness across cemented deposits of varying ages and have an abrupt basal boundary, indicating that they are distinct deposits and not entirely soil horizons. On the basis of soil development and stratigraphic position, units 18 and 19 are dated at late Pleistocene and are tentatively correlated with unit Qa4 (table 20).

The uppermost deposits in trench SCF–T1 and the adjacent test pit (units 20–22, pl. 8) are composed of silty alluvial gravel, as much as 1 m thick. An alluvial origin for unit 20 is evidenced by imbricated gravel clasts. Soil development within these deposits consists of a thin vesicular A (Av) horizon, a minimal cambic (Bw) horizon, and $CaCO_3$ stage I–I+ morphology. Units 20 through 22 are dated at latest Pleistocene or early Holocene and are correlated with unit Qa5 (table 20).

Structure

The south wall of trench SCF–T1 (pl. 8) exposes a fault zone, almost 20 m wide, consisting, from east to west, of minor displacements within the tuff and basal gravel (stas. 4.5–6 m), a main bedrock-alluvium fault zone (stas. 9–13), a zone of subvertical fractures and fissures (stas. 15.5–20 m), and irregular antithetic faults (stas. 19.5–24 m). The entire fault zone may not be exposed; minor ruptures may exist farther downslope to the west, but additional large offsets are unlikely. Only one faulting event (ash-related event Y, tables 8, 22) is clearly evident at this site; other events are primarily slip events along the main fault zone. Because erosion apparently has removed some deposits, particularly on the footwall, preserved relations are insufficient to confidently determine a sequence of faulting events.

The main bedrock-alluvium fault contact is a 1- to 2-m-wide, west-dipping zone of laminar carbonate and cemented gravel (stas. 9–13 m, pl. 8) that is downfaulted along a planar bedrock fault striking N. 11° E. and dipping 50° NW. This main fault zone flares upward slightly and likely narrows at shallow depth. The uppermost deposits (units 19–22), the oldest of which (unit 19) contains argillic soil, extend undisturbed across the main fault zone. In trench SCF–T1, an animal burrow disrupts unit 19 near the fault zone, but this unit is clearly unfaulted where exposed in the adjacent test pit.

Slight topographic irregularities on the surface above the main fault zone were originally interpreted as small scarps resulting from offset of surficial deposits, although the small amount of offset is near the limit of resolution of such features. Three topographic profiles of the fan surface all show surface irregularities at the fault zone, but only the profile surveyed on an adjacent, older surface shows down-to-the-west surface offset. Two profiles surveyed adjacent to trench SCF–T1 on the unit Qa5 (table 20) surface indicate that drainage across the cemented gravel deposits was deflected by contrasts in competence at the fault zone, but do not show any vertical separation of the unit Qa5 surface.

Although fault/stratigraphic relations across the main fault zone are poorly preserved, owing to erosion, crosscutting relations place some constraints on fault history. The most recent displacement (on the basis of the thickness of a small wedge of largely unconsolidated gravel, silt, and colluvial material within the main fault zone where all the other fill deposits are strongly cemented) is considered to have been at least 30 cm and to have occurred in late Quaternary time but before the development of the unfaulted argillic soil in unit 19 (pl. 8). Correlation of this displacement with the faulting events discussed above for trench T8 is uncertain; however, the most recent event (min 15±4 ka) interpreted for trench T8 (sample HD 1071, table 21) probably postdates unit 19 in trench SCF–T1.

The alluvial-gravel deposits (units 5–8, pl. 8) that contain the upper petrocalcic horizon with $CaCO_3$ stage IV morphology are progressively downthrown against the main fault; the surface of unconformity overlain by unit 5 is displaced about 1.5 m. This offset may be a minimum, owing to an unknown amount of erosional stripping of the footwall, but conversely, displacement may be exaggerated by backtilting. The offset of units 5 through 8 apparently occurred during mid-Quaternary to late Quaternary time, because cementation indicates these deposits to be no older (approx 900 ka; see below) than the deposits exposed in trench SCF–T3 (fig. 34). If this displacement occurred during the mid-Quaternary to late Quaternary, as is believed to be likely, then the small wedge of unconsolidated material within the fault zone that was mentioned above was deposited later. The offset across the main fault zone occurred in addition to that associated with the basaltic-ash-filled fissures (see below), which are downslope to the west (stas. 16.5–19.5 m, pl. 8). Units 5 through 8 unconformably overlie the lowermost exposed deposits (units 1–4), which are backtilted and displaced along a fault plane that is truncated by unit 5, indicating an even older displacement (of unknown age) across the main fault zone.

Trench SCF–T1 (pl. 8) also exposes a broad zone of hanging-wall deformation. A 4-m-wide zone of subvertical faults, fractures, and fissures (stas. 15.5–19.5 m, pl. 8) is largely engulfed in carbonate but also includes two conspicuous basaltic-ash-filled fissures. The eastern fissure (stas. 16.5–17 m) has a slight westward dip (85° NW.) and strikes nearly parallel to the main fault zone (N. 15° E.), whereas the western feature (sta. 19 m, pl. 8) strikes about 15° oblique to the main fault zone (N. 30° E.) and is nearly vertical. These two fissures cut the same deposits (units 1–8) and contain similar amounts of secondary carbonate; therefore, they are

assumed to represent the same faulting event. The western fissure contains reworked B-horizon peds, indicating that soil horizons, which may have been present at the time of faulting, were subsequently stripped. No direct measurements of surface offset related to these fissures are possible, owing to subsequent surface erosion, but the total width of the fissure opening (30–60 cm) indicates dip slip of 50 to 90 cm. If the small wedge of unconsolidated fill deposits within the main fault zone possibly relates to the same faulting event (Y, table 22), displacement caused by this single event may have ranged from 80 to 120 cm.

Cumulative displacement across the entire fault zone exposed in trench SCF–T1 (pl. 8) is uncertain. However, considering the displacement associated with the ash-filled fissures discussed above, the offsets on the main fault zone, the minor offset in the footwall, and possible backtilting, the cumulative mid-Quaternary to late Quaternary dip slip is estimated at 1.6 to 2.4 m.

West of the zone of subvertical fractures and fissures are several minor offsets and openings along antithetic (east dipping) faults with varying but shallow-dipping orientations. Basaltic-ash-filled openings within this zone strike oblique to,

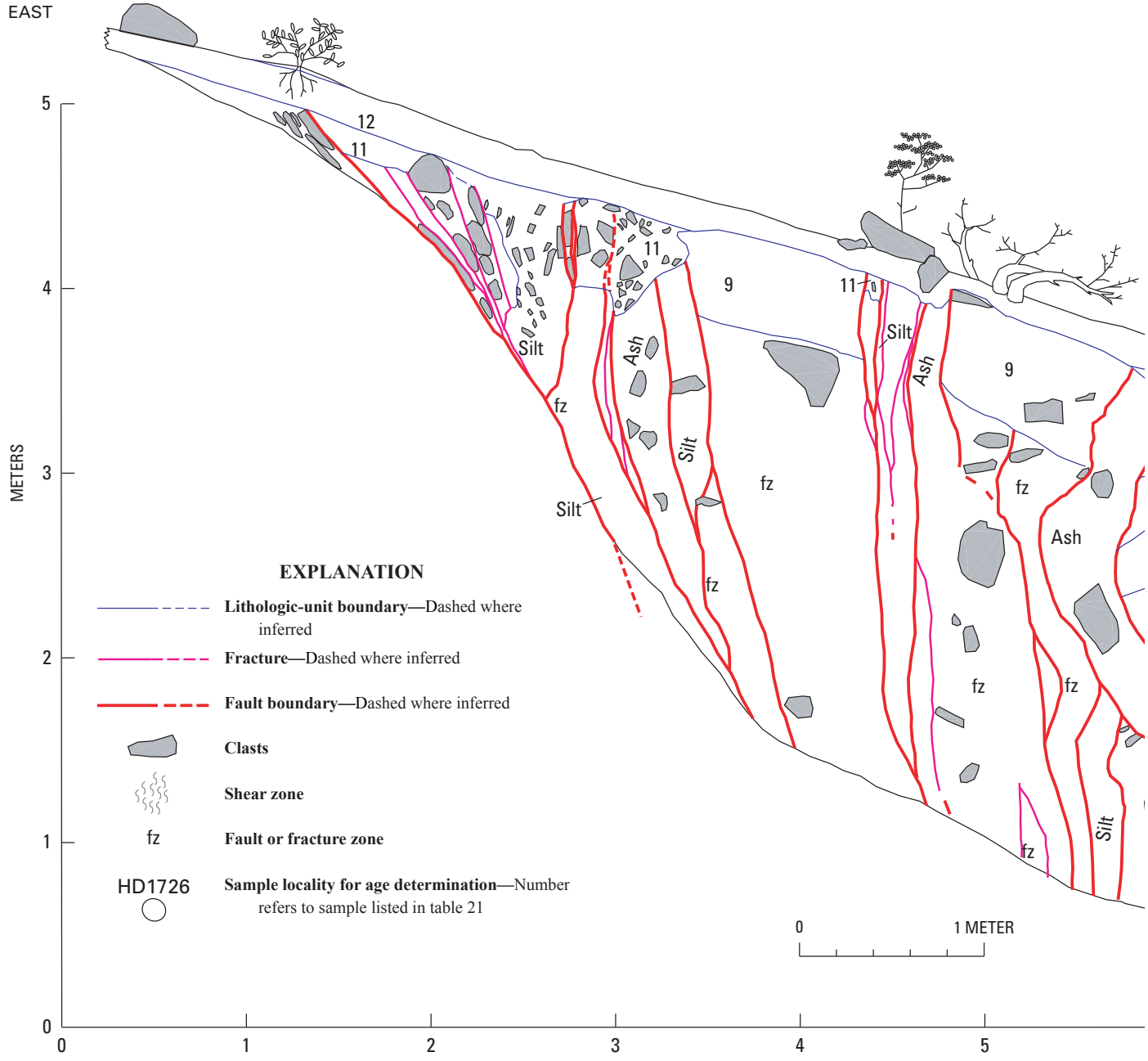

and dip into, the trench wall; these features are absent in the north wall of the trench.

Although the geologic relations exposed in trench SCF–T1 are not definitive enough for reliably determining offsets or numbers and dates of faulting events, several comparisons with the deformation in trench T8 are possible. The most recent faulting event evident in trench T8 is not observed in trench SCF–T1, other than possibly being represented by cemented fractures cutting the ash-filled fissures. The relatively large ash-related faulting event (Y, table 22) involved a fissure opening comparable to that at trench T8, indicating a similar offset. The estimated total displacement (approx 2 m) is reasonably similar to the estimated cumulative offset for trench T8. The presence of carbonate-cemented ($CaCO_3$ stage V morphology) gravel near the surface on the hanging wall of the Solitario Canyon Fault supports the interpretation that a hiatus in fault activity preceded the observed mid-Quaternary to late Quaternary events.

Trench SCF–T3

Trench SCF–T3 (figs. 2, 34) is located on an eroded remnant of hillslope colluvium, about 700 m north of trench SCF–T1 (fig. 2). The trench was located so as to possibly

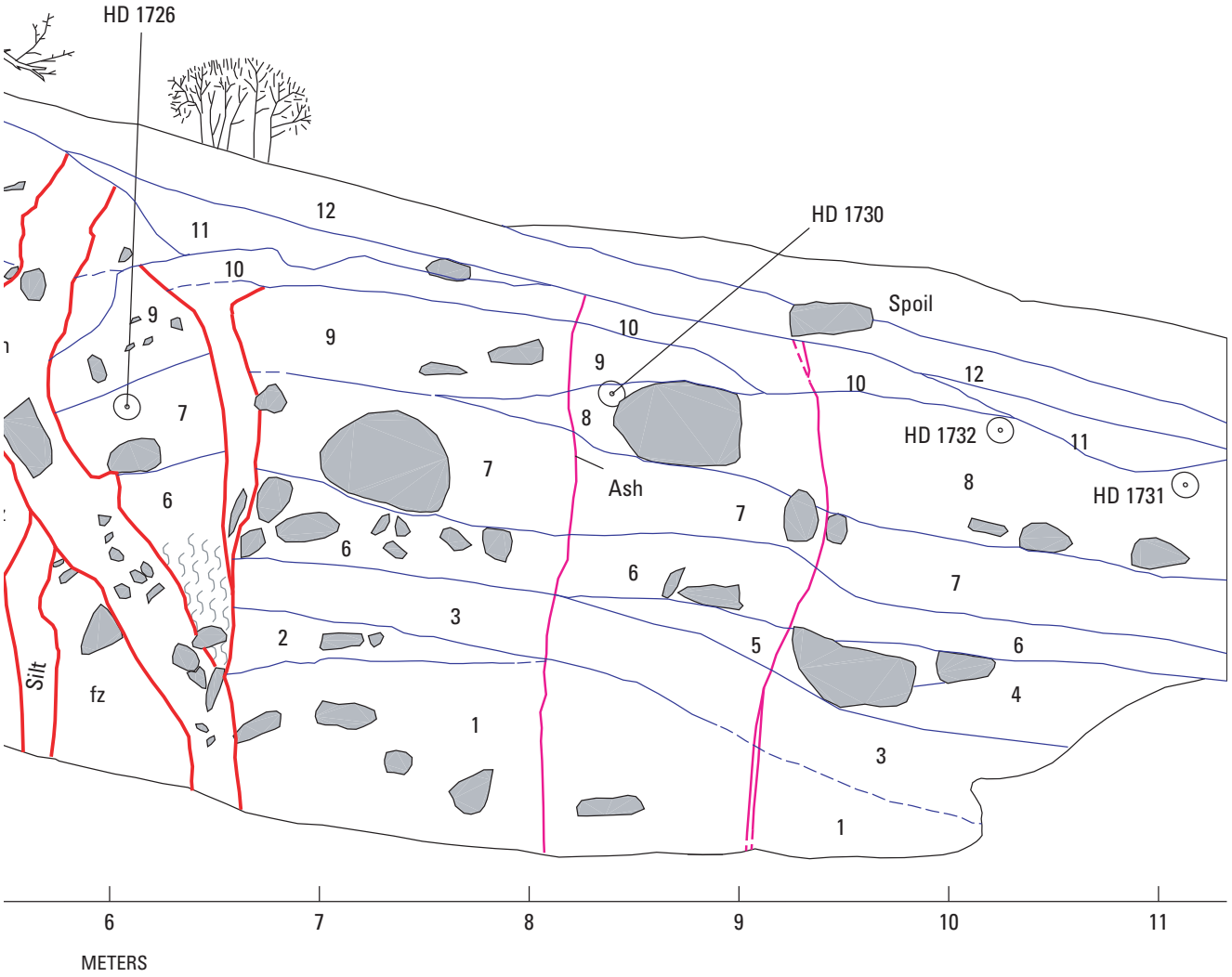

Figure 34. Log of south wall of trench SCF–T3 across the Solitario Canyon Fault in the Yucca Mountain area, southwestern Nevada (figs. 1, 2). See table 20 for correlation of map units.

provide a more complete record of faulting events than that observed in trenches T8 and SCF–T1.

Stratigraphy

Trench SCF–T3 (fig. 34) exposes hillslope and colluvial deposits downthrown against welded tuff of the Topopah Spring Tuff across the Solitario Canyon Fault. The colluvial deposits compose three distinct packages, each with a distinctive soil development. The two older units, which are moderately to extremely well cemented by silica and carbonate, are limited to the downthrown side of the fault. The upper soil horizons associated with the upper petrocalcic horizon have been stripped by erosion. The bedrock is present basically at the ground surface on the upthrown side of the fault. A thin (10–30 cm thick) deposit of Holocene colluvium and eolian silt overlies both the cemented colluvial deposits and the tuff.

The lowermost deposits (units 1, 2, fig. 34) in trench SCF–T3 are well cemented by silica and carbonate and appear to be truncated by a buried soil horizon (unit 3). The extensive silica and carbonate ($CaCO_3$ stage III–IV morphology) accumulation has largely obliterated the original sedimentary fabric of these three deposits, making both the defined stratigraphic contacts and buried soil horizons uncertain. On the basis of extensive silica and carbonate accumulation and stratigraphic position, units 1 and 2 are dated at early Pleistocene and are correlated with the oldest Quaternary deposits (unit Qa1, table 20) generally present in the Yucca Mountain area (figs. 1, 2).

Units 4 through 9 (fig. 34) also are entirely engulfed in carbonate, and most of the original sedimentary fabric is obliterated, indicating considerable antiquity. Silica-rich clast rinds in units 7 and 8 (samples HD 1726, HD 1730, HD 1731, HD 1732, fig. 34, all from large boulders) yielded a wide range of U-series ages, many older than 500 ka (table 21). On the basis of extensive silica and carbonate ($CaCO_3$ stage III–V morphology) accumulation, units 4 through 9 are dated at early to middle Pleistocene and are also correlated with the oldest Quaternary deposits (unit Qa1, table 20) generally present in the Yucca Mountain area (figs. 1, 2).

Unit 10 (fig. 34) is a thin, well-cemented ($CaCO_3$ stage IV morphology) colluvial deposit present on the downthrown side of the fault zone. The material may have been deposited in response to surface faulting. The original upper soil horizons associated with the accumulated carbonate have been stripped. Because this deposit appears to be localized and numerical-age control is absent, unit 10 cannot confidently be correlated with other units; however, the deposit is crosscut by the larger of two ash-filled fissures, a relation that, in combination with the amount of carbonate accumulation in the unit, indicates an age older than about 80 ka.

The uppermost deposits (units 11, 12, fig. 34) in trench SCF–T3 consist of silty gravel composed of eolian silt and colluvium. In the western part of the trench (west of sta. 9 m, fig. 34), unit 12 was disturbed during excavation. Soil development within these deposits consists of a fairly thin vesicular A (Av) horizon, minimal cambic (Bw) horizon, and $CaCO_3$ stage I–I+ morphology. Units 11 and 12 are dated at latest Pleistocene to early Holocene and are probably correlated with unit Qa5 (table 20).

Structure

Trench SCF–T3 (fig. 34) exposes a 3- to 5-m-wide fault zone bounded on the east by a bedrock fault plane dipping 62° W. (fig. 34). The fault zone, consisting largely of laminar or massive carbonate and carbonate-cemented gravel, includes several subvertical gravel- and ash-filled fissures and cemented fractures. The exposed relations indicate that the fault zone narrows at a shallow (<10 m) depth. The extensive carbonate accumulation has obscured much of the older fault fabric. Mid-Quaternary to late Quaternary faulting is evidenced by fissures filled with gravel, silt, and basaltic ash. Older carbonate-cemented gravel within the fault zone was likely emplaced in similar subvertical fissures.

The uppermost deposits (units 11, 12, fig. 34), consisting of mixed colluvium and eolian silt, do not appear to be faulted. Silt (unit 11) fills three openings: (1) a 30-cm-wide opening (sta. 2.5 m, fig. 34) that extends upward from the bedrock fault plane, (2) a uniform opening of a few millimeters along the bedrock/fault-zone contact (sta. 3 m), and (3) a narrow fracture within the carbonate-engulfed fault zone (sta. 4.3 m). Although these narrow openings may have resulted from minor fault-related extension, they do not appear to have been caused by measurable fault displacement. The 30-cm-wide opening is interpreted to be an erosional feature because, if it were fault related, an offset creating a much more noticeable scarp than is apparent in the exposure would be required, as well as slip along the bedrock fault plane, which also is not apparent.

Carbonate-filled fractures that cut and disturb an ash-filled fissure (stas. 3–3.5 m, fig. 34; see next paragraph) indicate that at least one fracturing event postdated the large ash-related event. Presumably, this fracturing event is equivalent to the most recent faulting event observed in trench T8 (fig. 2). No displacement associated with this event was measurable in trench SCF–T3.

Two fissures in trench SCF–T3 (fig. 34) contain abundant basaltic ash throughout their exposed vertical extents. Both fissures cut all but units 11 and 12 (fig. 34). The larger fissure (stas. 5.5–6.5 m, fig. 34) is filled mostly with gravel that has a basaltic-ash matrix. The smaller fissure (stas. 3–3.5 m, fig. 34) contains more ash than gravel clasts. Both fissures cut similar-age deposits, have similar ash contents, and contain similar secondary carbonate; accordingly, the two fissures are inferred to have formed during a single faulting event (Y, table 22). Although the offset associated with this event was not directly measurable, the combined fissure width (30–60 cm) indicates dip slip of 0.6 to 1.2 m. At the top of the petrocalcic horizon, both ash-filled fissures are erosionally truncated and buried by Holocene silt and colluvium, probably reflecting early Holocene stripping of the upper soil horizons down to the more resistant petrocalcic horizon.

An uncemented gravel- and silt-filled fissure (sta. approx 5.5 m, fig. 34) that is crosscut by the western ash-filled fissure contains minor basaltic ash in its upper part and may reflect an earlier ash-related faulting event, although reworking of ash from the younger crosscutting fissure is also possible. This earlier faulting event may be associated with the fault-related features (possible colluvial wedge [unit 10] and backtilted gravel) present at about station 6 m (fig. 34), which are much more cemented by carbonate than is the ash-filled fissure. This feature probably was formed during event W as observed in trench T8, but such an association would be difficult to substantiate. Except where cut by the two zones of late Quaternary fissuring, the uppermost well-cemented colluvial deposit (unit 9) extends across the fault zone, truncating older fault features and apparently representing a significant mid-Quaternary hiatus in seismicity. Faulting events predating unit 9 are evidenced by juxtaposition of older deposits against the fault zone, by a distinct fault contact within the fault zone (sta. 4.3 m, fig. 34), and by a carbonate-cemented fissure (sta. 5.3 m, fig. 34).

Although the juxtaposition of colluvial deposits against bedrock at the east end of trench SCF–T3 (fig. 34) precludes any direct measurement of fault displacements, displacements can be estimated on the basis of the position of deposits on the hanging wall. For example, the displacement of unit 9 can be estimated from the vertical separation between the base of units 11 and 12 (top of bedrock on the footwall) and the top of unit 9 on the hanging wall, which is about 60 to 70 cm (dip slip, 80–90 cm), assuming that a comparable thickness of unit 9 was eroded off the footwall after displacement occurred. Assuming that older units in the hanging wall also were deposited across the fault and rested on the bedrock surface of the footwall, displacements are estimated at about 1.6 m for units 6 and 7 and about 2.8 m for units 1 and 2.

Trench SCF–T4

Trench SCF–T4 (pl. 9) is the northernmost of the trenches spanning the Solitario Canyon Fault that is discussed in this chapter (fig. 2). The trench was excavated into an eroded remnant of hillslope colluvium to investigate the fault activity at a locality close to the west side of the proposed repository site for the storage of high-level radioactive waste storage at Yucca Mountain (fig. 1).

Stratigraphy

Trench SCF–T4 (pl. 9) exposes hillslope and fault colluvium downthrown against welded and nonwelded tuff of the Paintbrush Group (Day and others, 1998b). The nonwelded tuff, which fills a sliver between two principal fault strands, forms the footwall of the upper (eastern) fault strand. The older colluvial deposits (units 1–7) in the hanging wall are moderately to well cemented by silica and carbonate; the upper soil horizons associated with the petrocalcic horizons in these deposits have been erosionally stripped. The cemented colluvium and bedrock tuff are buried by deposits of less well indurated colluvium and eolian silt (units 8–10) of varying thickness.

The lowermost deposit (unit 1, pl. 9) exposed in trench SCF–T4 is well cemented by silica, indicating, in combination with its stratigraphic position, an early Pleistocene or older age (probably >1 Ma); the deposit may even be silicified bedrock.

Unit 1 is overlain by several hillslope colluvial deposits (units 2–6), the lower of which (units 2–4) are only moderately cemented ($CaCO_3$ stage II morphology), whereas the upper deposits (units 5–6) contain a well-developed petrocalcic horizon ($CaCO_3$ stage III–IV morphology). This contrast in cementation indicates that the upper units were deposited and subsequently plugged by soil development before much carbonate had accumulated in the lower units. Unit 4 pinches out downslope from the main Quaternary fault zone, indicating that the unit is a colluvial wedge related to surface faulting. On the basis of extensive silica and carbonate accumulation ($CaCO_3$ stage II–IV morphology), though somewhat less than that in the unit Qa1 deposits exposed in trenches T8, SCF–T1, and SCF–T3, units 2 through 6 are dated at early to middle Pleistocene (at least a few hundred thousand years to probably >500 ka) and are correlated with the oldest Quaternary deposits (unit Qa1, table 20) generally present in the Yucca Mountain area (figs. 1, 2).

Unit 7, which also thins downslope from the main fault zone (stas. 10–11 m, pl. 9), appears to be a small colluvial wedge deposited in response to faulting. The deposit is well cemented ($CaCO_3$ stage IV morphology), and the original upper soil horizons have been stripped. Unit 7 appears to be associated with the largest mid-Quaternary to late Quaternary faulting event (discussed below), which is dated at 80–60 ka. Although $CaCO_3$ stage IV morphology seems extreme for a deposit of this age, carbonate accumulation was likely accentuated by the position of the deposit at the base of a bedrock hillslope.

Bedrock is overlain by a colluvial deposit (unit 8, pl. 9) containing a weak argillic (Bt) soil horizon. The unit was deposited on an eroded, irregular surface, resulting in a varying thickness. On the basis of soil development and stratigraphic position, unit 8 is dated at late Pleistocene and is correlated with either unit Qa3 or Qa4 (table 20).

The uppermost deposits (units 9, 10) are composed of mixed colluvium and eolian silt. Soil development within these deposits is minimal, consisting of a fairly thin vesicular A (Av) horizon with $CaCO_3$ stage I morphology. On the basis of soil development, units 9 and 10 are tentatively dated at early Holocene through latest Pleistocene and are correlated with unit Qa5 (table 20).

Structure

Trench SCF–T4 (pl. 9; fig. 2) exposes two fault zones (stas. 5, 10.5 m, pl. 9), both of which are about 1 m wide and contain laminar and massive carbonate and brecciated and silicified tuff. The eastern fault zone separates welded tuff

(to the east) from nonwelded tuff (to the west), whereas the western fault zone separates nonwelded tuff from colluvial deposits on the hanging wall. The dips of these two fault zones (65° and 85° W.) indicate that they probably merge at shallow depth (10–15 m below the ground surface), and that the western fault zone likely splays subvertically from a west-dipping bedrock fault. Mid-Quaternary to late Quaternary activity is evidenced by at least three subvertical fissures separating the western fault zone from the hanging-wall deposits; one of these fissures is truncated by, and therefore predates, the upper petrocalcic horizon. No definitive evidence of Quaternary activity was observed along the eastern fault zone.

The largest fissure exposed in trench SCF–T4 (sta. 10.5 m, pl. 9) contains abundant basaltic ash and is cut by carbonate-filled fractures. The fractures may have formed contemporaneously with the most recent faulting event that is apparent at trench T8, but no radiometric ages are available to corroborate such a correlation. No offset was detected on these fractures in the trench. The basaltic-ash-filled fissure at station 10.5 m (pl. 9) widens upward from about 10 cm at the floor of the trench to about 20 cm at its uppermost extent. This fissure is overlain by a small colluvial wedge (unit 7) deposited against the fault zone on a backwasting scarp on the hanging wall. Similarities with the ash-filled fissures exposed at other trench sites along the Solitario Canyon Fault indicate that all of the fissures formed during the same faulting event.

The displacement associated with the ash-filled fissure in trench SCF–T4 (pl. 9) is not directly measurable, because no displaced units can be matched across the fault; however, the offset can be estimated from the maximum thickness of the unit 7 colluvial wedge (15–30 cm, depending on the amount of erosional backwasting into the fissure), the fissure width (10–20 cm), and the vertical separation (10–25 cm) of the base of units 8 through 10. The colluvial wedge provides a minimum estimate of the vertical offset; here, no erosional beveling of the footwall is evident, and so the wedge thickness may closely approximate the actual vertical offset. The upward widening of the ash-filled fissure and east-dipping fractures indicates deformation and tilting of the hanging wall, contributing uncertainty to estimates of offset based on fissure widths. Although each of these lines of evidence is relatively weak by itself, they all indicate dip slip of 20 to 40 cm (event Y, table 22).

A narrow (≤10 cm wide), well-cemented fissure (sta. approx 10.5 m, pl. 9) bounds the west side of the ash-filled fissure and cuts the upper petrocalcic horizon (units 5, 6). This fissure, which is truncated by erosional backwasting into the ash-filled fissure, is inferred to have formed during the same faulting event as that which created the second-largest fissures in trenches T8 and SCF–T3. Although the offset associated with this event is not measurable, the fissure width indicates an offset of about half that associated with the ash-filled fissure.

Fault relations observed in trench SCF–T4 (pl. 9), as well as the relatively small fault scarps along this segment of the Solitario Canyon Fault, indicate that the displacements here are much less than those displayed at the other trench sites. Estimated cumulative dip slip, based on the apparent downthrow of units 5 and 6, is 60 to 80 cm during mid-Quaternary to late Quaternary time (table 22). At least three episodes of earlier faulting are also indicated in the trench exposure, but data are insufficient for estimating displacements. A substantial structural discontinuity along the Solitario Canyon Fault exists between trenches SCF–T4 and T8, about where the Iron Ridge Fault splays off from the main fault trace (Day and others, 1998a). This discontinuity may have inhibited northward propagation of some ruptures and arrested some smaller events.

Trench SCF–T2

Trench SCF–T2 (pl. 10; fig. 2) was excavated across a scarp in an eroded remnant of hillslope colluvium at the base of the large west-facing escarpment formed by the Iron Ridge Fault, the main eastern splay of the Solitario Canyon Fault. The Iron Ridge Fault trends toward, and may extend far enough to intersect, the Stagecoach Road Fault to the south (Simonds and others, 1995). The trench was excavated to evaluate the paleoseismic history of the Iron Ridge Fault and thereby to assess the fault as a possible link between the Solitario Canyon and Stagecoach Road Faults.

Stratigraphy

Trench SCF–T2 exposes hillslope and fault-scarp colluvium downthrown against welded tuff of the Topopah Spring Tuff (pl. 10). The lowermost colluvial deposit (unit 1) is well cemented by silica and carbonate ($CaCO_3$ stage III–IV morphology). The deposit is exposed only near the bottom of the trench and is therefore difficult to examine in detail, but it appears to contain a buried soil horizon that was downthrown and remained relatively undeformed. Carbonate-filled fractures (2–3 cm wide) are truncated at the top of this deposit, indicating a substantial age difference with the overlying deposits. On the basis of extensive soil development and stratigraphic position, unit 1 is dated at probably early Pleistocene and is correlated with the oldest Quaternary deposits (unit Qa1, table 20) generally present in the Yucca Mountain area (figs. 1, 2).

Unit 1 (pl. 10) is overlain by colluvial deposits that thin markedly to the west, downslope from the fault; these deposits, especially the lower ones, are composed of at least some fault-scarp debris deposited in response to surface displacement along the Iron Ridge Fault. Unit 2 and the lower part of unit 3 have only moderate carbonate accumulation ($CaCO_3$ stage II morphology), whereas most of unit 3 and all of unit 4 contain a well-developed petrocalcic horizon ($CaCO_3$ stage III–IV morphology) that continues downslope into the overlying deposits. Units 2 through 4 are buried by hillslope colluvium (units 5, 6) that reflect a period of regrading and smoothing of the hillslope; units 4 and 5 are erosionally truncated. On the basis of soil development, units 2 through 6 are dated at middle Pleistocene or older (probably >500 ka) and are also

correlated with the oldest Quaternary deposits (unit Qa1, table 20) generally present in the Yucca Mountain area (figs. 1, 2).

Unit 7 (pl. 10), the uppermost deposit containing a strong petrocalcic horizon, also thins markedly downslope (pl. 9). The deposit may be composed of fault-scarp colluvium, but it is so eroded that its origin is obscure. Unit 7 is dated at middle Pleistocene or older and is also correlated with unit Qa1.

Units 8 and 9, which unconformably overlie units 4 through 7, are hillslope colluvial deposits that further regrade the slope and display noticeably less soil development than the underlying deposits. On the basis of carbonate accumulation ($CaCO_3$ stage II+ morphology), units 8 and 9 are dated at late Pleistocene and are tentatively correlated with unit Qa4 (table 20).

The uppermost deposits in trench SCF–T2 (units 10, 11, pl. 10) are composed of mixed colluvium and eolian silt. These deposits, especially unit 11, were disturbed during excavation in the western part of the trench. Soil development consists of a vesicular A (Av) horizon, a cambic (Bw) horizon, and $CaCO_3$ stage I morphology. Units 10 and 11 are dated at latest Pleistocene to early Holocene and are correlated with unit Qa5 (table 20).

Structure

Trench SCF–T2 (pl. 10; fig. 2) exposes a relatively narrow fault zone composed largely of laminar silica and carbonate deposits. Where it cuts unit 1, the fault zone is only partly exposed but appears to be about 60 cm wide; where it cuts units 2 through 4, it is about 30 cm wide. In addition to the main fault zone, a 2-m-wide fracture zone within the hanging wall is also exposed. Although stratigraphic relations are obscured by carbonate overprinting, the exposure provides at least general constraints on Quaternary activity along the Iron Ridge Fault.

A 2- to 3-cm-wide extensional opening (sta. 1.4 m, pl. 10) within the main fault zone extends with uniform width to at least 1-m depth (the limit of its exposure) and is filled with silt and fragmented carbonate. This feature could represent a minor faulting event (dip slip, possibly 5–10 cm) of probable Holocene age. Fractures in the uppermost deposits (units 10, 11) and a possible small scarp (approx 10 cm high) indicate that this faulting event postdates the youngest exposed deposits. Units 10 and 11, however, are composed largely of eolian silt, which is dynamic under wet/dry cycles; the observed fracturing could therefore be a secondary effect not directly related to faulting.

Direct evidence of offsets associated with mid-Quaternary to late Quaternary activity along the main Solitario Canyon Fault trace is absent. Only fractures and possible minor offsets, including the silt-filled opening discussed above, cut the petrocalcic horizon formed in units 3 and 4 (pl. 10). The apparent step in unit 9 (sta. approx 3.3 m, pl. 10) appears to be erosional because the fracture across it does not appear to displace lower, older features. The petrocalcic horizon in units 3 through 7 closely grades to the bedrock hillslope above the trench, and so large displacements subsequent to the formation of this soil horizon probably did not occur.

The most significant Quaternary fault activity evident in trench SCF–T2 (pl. 10) predates the petrocalcic horizon in units 3 through 7 and therefore is dated at middle Pleistocene or older. The colluvial-wedge deposits (units 2–4) and soil relations (petrocalcic horizon superimposed on both fault-scarp and hillslope colluvium) provide possible evidence that the observed fault displacement occurred as an episode of elevated activity, rather than as long-term, recurrent activity. The displacement involved can only be approximated; erosional truncation of cemented deposits on the downthrown side of the fault indicates a possible displacement of about 2 m. Preevent displacements of about 70 cm may also have occurred, on the basis of the apparent thicknesses of units 2 through 4, but the stratigraphic relations are too obscure for reliable estimates. Still-older activity is indicated by the wider fault zone and carbonate-filled fractures within unit 1, but the exposure is too limited for dating or estimating displacement.

Summary of Mid-Quaternary to Late Quaternary Activity on the Solitario Canyon Fault

The trenches examined during this study indicate a sequence of mid-Quaternary to late Quaternary surface-rupturing paleoearthquakes on the Solitario Canyon Fault that are manifested primarily as extensional fissures filled with gravel, silt, and basaltic ash. At least two, possibly as many as four, faulting events displace alluvial and colluvial gravel ranging in age from a few hundred thousand years to almost 1 Ma, indicating that the mid-Quaternary to late Quaternary activity was preceded by a fairly lengthy hiatus in seismicity.

The central trenches (T8, SCF–T3, SCF–T1) expose a largely singular fault trace, with an average strike of about N. 5° E. and a dip of 50°–60° W. Predominantly normal dip slip has displaced bedrock that is extensively exposed in the area (Tiva Canyon and Topopah Spring Tuffs of the Paintbrush Group) by an estimated maximum displacement of about 500 m (Day and others, 1998a). A subordinate component of left-lateral slip is indicated by bedrock striations in various places along the fault trace (rakes generally ranging from 50° to 70°; Simonds and others, 1995), but no evidence was observed as to whether these striations represent Quaternary displacements.

In the shallow exposures afforded by the trenches, Quaternary surface ruptures appear primarily as subvertical fissure openings that sole into a dipping bedrock fault plane. Secondary silica and carbonate accumulations along fractures and within fissure-fill material form a flaring-upward zone of laminar and massive carbonate and cemented gravel. The largest mid-Quaternary to late Quaternary fissuring events are clearly defined by gravel infilling within the

fault zone; earlier fissuring events are difficult to recognize because of carbonate overprinting. Additional minor fissuring is indicated by small displacements and (or) fracturing.

Total displacements associated with mid-Quaternary to late Quaternary activity on the Solitario Canyon Fault are not directly measurable because no offset stratigraphic markers can be reliably matched across the fault zone; only the uppermost, unfaulted deposits are present on both sides of the fault. However, offsets can be estimated from the downthrow of hanging-wall deposits, the vertical separation of erosional unconformities, and fissure widths (table 20). For example, offsets can be estimated from the fault dip and horizontal extension inferred from fissure widths, on the basis of the simple geometric model shown in figure 33. For the relatively large, ash-filled fissure exposed in trench T8 (fig. 31), which has mostly planar walls and a uniform width to where it narrows against the bedrock fault (indicating minimal hanging-wall deformation), this method yields a reasonably accurate dip-slip estimate of 1.1 to 1.3 m. Where fissures narrow and do not extend to the bedrock fault plane, however, uncertainties are relatively large.

Continuity of the fault scarp through trenches T8, SCF–T3, and SCF–T1 indicates that these trenches record similar faulting histories; the record of mid-Quaternary to late Quaternary surface ruptures within each trench appears to be reasonably consistent, at least for the largest faulting events. Minor surface breaks associated with moderate ($M \leq 6.5$) earthquakes are typically discontinuous (for example, dePolo, 1994); any smaller faulting events are thus unlikely to correlate between trenches. At trench SCF–T4 (pl. 9), on the northern section of the Solitario Canyon Fault, the two largest mid-Quaternary to late Quaternary surface ruptures appear to correlate with events on the central section of the fault, but only carbonate-filled fractures provide any possible evidence for smaller events. Preliminary observations in trench SCF–E1 (fig. 2), an excavated natural wash exposure across the southern section of the Solitario Canyon Fault, indicates that displacement is substantially less there than along the central section of the fault, confirming similar observations based on a relatively small scarp in mid-Quaternary deposits. The mid-Quaternary to late Quaternary activity along the Solitario Canyon Fault does not correlate with activity along the Iron Ridge Fault.

Sequence of Faulting Events

The following outline of the sequence of faulting events (youngest to oldest) on the Solitario Canyon Fault is based largely on the geologic relations observed along the south wall of trench T8 (fig. 31), where the most complete record of mid-Quaternary to late Quaternary surface ruptures is exposed and the largest offsets occurred. We emphasize that such observations and interpretations apply only to a limited section of this 18-km-long fault and are not necessarily characteristic of its entire extent. Individual faulting events are correlated between trenches as the available evidence permits.

Fracturing Events

Two fracturing events postdate the most recent well-defined faulting event (Z, table 22). The youngest fracturing event is indicated by silt-filled fractures exposed in trenches T8, SCF–T3, and SCF–T2, but no associated fault displacement is distinguishable at any of these sites. The absence of carbonate accumulation in these deposits indicates a Holocene age. A somewhat earlier fracturing event is evidenced by a silica- and carbonate-filled fracture in trench T8 that cuts all cemented deposits, including those that overlie and postdate event Z. Although similar fracturing was not observed at the other trench sites, conditions were unfavorable for preserving such evidence. The origin of the fractures is uncertain; they could have been caused by moderate earthquakes on the Solitario Canyon Fault, or they may be related to earthquakes on other nearby or regional faults. Alternatively, they could have a nontectonic origin (for example, bioturbation), although similar fractures exposed in washes throughout eastern Crater Flat are spatially associated with known Quaternary faults (Ramelli and others, 1989).

Event Z

The most recent, well-defined episode of fault displacement (event Z, table 22) is expressed in trench T8 (figs. 31, 32) by carbonate-filled fractures that cut the basaltic-ash-filled fissure (represented by event Y), by ash dragged along the fault, and by a narrow (10–15 cm wide) silt- and ash-filled fissure exposed in the north trench wall of the trench (fig. 32). On the basis of the geometry shown in figure 33, these features indicate an offset of 10 to 20 cm during this faulting event, conceivably reflecting afterslip associated with event Y, but interpreted to have occurred during a subsequent faulting event. The presence of ash may be interpreted to indicate that event Z was associated with eruptive activity at the nearby Lathrop Wells volcanic center, but considering the age of the ash associated with event Y, reworking of ash into this younger fissure is a more reasonable explanation.

In trenches SCF–T3, SCF–T1, and SCF–T4, possible evidence for event Z is in the form of carbonate-filled fractures that crosscut and (at trenches SCF–T3 and SCF–T4) appear to disturb the conspicuous ash-filled fissures, but no displacements are discernible. In trench SCF–T1, a small colluvial wedge deposited against the main fault zone (unit 17; sta. 10.5 m, pl. 8) and the loose silt- and gravel-filled zone within the main fault zone could relate to event Z, but soil development in the overlying, unfaulted deposits is probably older. Event Z is not apparent at trench SCF–T2, located on the Iron Ridge Fault. Various expressions of event Z among the trench sites indicate displacements ranging from 0 to 20 cm, probably averaging 10 cm.

An average U-series age of 15.5±4.3 ka on fracture-filling carbonate (sample HD 1071, table 21) associated with the dragged ash provides a possible minimum date for event Z. Although a maximum date is difficult to define, the event

probably postdates the secondary carbonate (sample HD 1070) within the event Y fissure (U-series age, 27–56 ka). Event Z is dated at 40–20 ka (preferred value, 30–20 ka).

Event Y

The four trenches across the Solitario Canyon Fault expose conspicuous fissures containing abundant basaltic ash. At each site, these ash-filled fissures represent the largest mid-Quaternary to late Quaternary surface ruptures and exhibit similar characteristics; they are therefore assumed to represent a single faulting event, penultimate event Y, which is expressed at trench T8 as a conspicuous 60- to 70-cm-wide fissure with planar walls. On the basis of a simple geometric model (fig. 33), that assumes rigid behavior of the hanging-wall block, the displacement associated with event Y is dip slip of 1.1 to 1.3 m (0.9–1.1 m of vertical displacement).

Event Y probably created the two conspicuous ash-filled fissures in trench SCF–T3 (fig. 34). Although the absence of offset stratigraphic markers makes any direct measurement of displacement difficult, the cumulative fissure width (30–60 cm) is interpreted to indicate a possible dip-slip displacement of 0.6 to 1.2 m (table 22). The uppermost value (1.2 m) may be an overestimate because the wider openings at the top of the fissures could be accentuated by tilting. Vertical separation (0.6–1.0 m) of the top of the petrocalcic horizon indicates cumulative mid-Quaternary to late Quaternary dip slip of 0.8 to 1.3 m.

Event Y is represented in trench SCF–T1 (pl. 8) by three ash-filled fissures in the hanging wall, two of which are subvertical, whereas the third is a minor, low-angle splay that dips into the south wall of the trench at an apparent angle much lower than its true dip. The cumulative width of the three ash-filled fissures is difficult to determine, especially considering the low-angle inclination of the third fissure, but is estimated at 25 to 50 cm, indicating dip slip of 40 to 80 cm. Owing to subsequent erosion, vertical separation of the former ground surface is not measurable.

Event Y is expressed in trench SCF–T4 (pl. 9) by a single ash-filled fissure whose width (10–20 cm) indicates a relatively small displacement (20–40 cm, table 22). Vertical separation of the assumed former ground surface and thickness of a colluvial wedge apparently associated with this faulting event yield similar estimated displacements.

At all the trench sites, ash-filled fissures are by far the most conspicuous surface ruptures cutting well-cemented alluvial and colluvial gravel ($CaCO_3$ stage III–V morphology). At trenches SCF–T1 and SCF–T3 (fig. 2), these gravel deposits are extremely well cemented ($CaCO_3$ stage V morphology), and a U-series age of 950±140 ka from trench SCF–T3 (sample HD 1726, table 21) indicates that the deposits may be as old as 1 Ma. Considerably less cementation of the gravel deposits was observed in trenches T8 and SCF–T4, and at least in trench T8 these deposits are probably no older than about 200 ka, on the basis of correlation with unit Qa3 (tables 2, 20).

A date of several tens of thousands of years before present for event Y (table 8) is indicated by a fairly well developed soil in the upper part of a fissure fill in trench T8 (figs. 31, 32) and in a cobbly-silt deposit capping the fissure. Thin silica and carbonate laminae are spaced throughout the upper 1 m of these deposits. U-series ages of 27–56 ka on secondary carbonate (sample HD 1070, table 21) and 114–124 ka on fracture-filling carbonate (sample HD 1072) provide minimum and maximum dates, respectively, for event Y. The closest approximation is considered to be the age of the basaltic ash, which is correlated with an eruption of the nearby Lathrop Wells volcanic center (fig. 1) at 77±6 ka (Heizler and others, 1999).

Event X

In trench T8, a relatively small faulting event is indicated by an apparent gravel-filled fissure sandwiched between events W and Y fissures (sta. 3.5 m, fig. 31). This well-cemented feature has a jumbled fabric, distinguishing it from the adjacent alluvial deposit (unit 9, fig. 31). A narrow gravel-filled fissure in trench SCF–T4 (pl. 9) may also reflect event X but is considered to be more likely related to event W, which is a larger and more pronounced feature at both trenches T8 and SCF–T3. Event X is problematic at trenches SCF–T3 and SCF–T1 but cannot be precluded at either site. Little information is available to constrain the offset associated with this possible faulting event; the width (approx 15 cm) of the apparent fissure in trench T8 approximates a dip-slip displacement of 20 to 30 cm. An average U-series age of 118±6 ka (sample HD 1072, table 21) on fracture-filling carbonate from trench T8 provides an apparent close minimum date for event X.

Event W

Event W is evidenced by fairly conspicuous fissures in trenches T8 (stas. 3.5–4 m, fig. 31) and SCF–T3 (sta. 5.5 m, fig. 34). The fissure in trench T8 extends as a narrowing-downward feature into older fault-zone carbonate in the western part of the fault zone. The fissure in trench SCF–T3, which is crosscut by the ash-bearing event Y fissure, contains silt, gravel, and minor basaltic ash; the presence of ash could reflect an episode of faulting and volcanism predating event Y, although the ash in the event W fissure could have been contaminated with event Y ash. The gravel-filled fissure bounding the west side of the ash-filled fissure in trench SCF–T4 probably also formed during event W. The date of event W is constrained by the estimated age (150–250 ka) of the deposits in trench T8 that were displaced by the faulting event, and by the average U-series age (118±6 ka) of the fissure fill apparently associated with event X.

Early Quaternary to Mid-Quaternary Hiatus in Seismicity

Well-cemented to extremely well cemented alluvium or colluvium is present at or very near the ground surface on the downthrown side of the Solitario Canyon Fault at all of the trench sites across it. The petrocalcic horizon within these

deposits is closely graded to the bedrock hillslope above the fault, indicating that before the mid-Quaternary to late Quaternary activity discussed above, little, if any, surface offset occurred over a period spanning several hundred thousand years. The U-series ages from trench SCF–T3 indicate that any significant earlier fault activity probably predates 900 ka.

Earlier Faulting

Despite the lengthy early Quaternary to mid-Quaternary hiatus in seismicity along the Solitario Canyon Fault, evidence does exist for earlier surface displacements. Precise ages and an event sequence for this earlier fault activity, however, are not definable from the available information. The fault activity indicated by the evidence described below should be considered a minimum for any activity that predates the sequence of mid-Quaternary to late Quaternary faulting events on the Solitario Canyon Fault.

Trenches T8 and SCF–T3 expose a well-developed fault zone that existed before mid-Quaternary to late Quaternary time, along which older gravel deposits (unit Qa1, tables 2, 20) are juxtaposed against bedrock. The main fault zone is an upward-thickening wedge separating the zone of vertical fissures from the bedrock fault plane. Evidence of individual events within the fault zone at these sites is largely obliterated by extensive silica and carbonate accumulation.

A gravel-filled fissure exposed in the south wall of trench T8 (sta. 2 m, fig. 31) indicates an earlier faulting event similar in magnitude to event W (table 8). The materials filling this older fissure are highly fractured and cut by 1- to 2-cm-thick silica veins but are not noticeably displaced. Similar, though less distinct, fractures were discerned within the fault zone in trench SCF–T3 (fig. 34). The degree of secondary silica and carbonate accumulation indicates a relatively early date for event W.

Earlier fault activity is best expressed in trench SCF–T1 (pl. 8), where the lowermost gravel deposits (units 1–4) are faulted and backtilted across a wider fault zone than that which cuts the overlying deposits (units 5–8). Trench SCF–T4 exposes evidence of at least three earlier faulting episodes, including a fissure capped by the upper petrocalcic horizon (possibly the same event as that recognized in trenches T8 and SCF–T3) and by an apparent colluvial wedge cut by that fissure.

The pre-late Quaternary fault activity on the Solitario Canyon Fault significantly predates eruptive activity at the nearby Lathrop Wells volcanic center (fig. 1); therefore, not all the Quaternary activity on the fault is explainable by the postulated association of faulting and volcanic activity for event Y.

Recurrence Intervals and Fault-Slip Rates

The occurrence of three or four faulting events over a time period of about 200 k.y. (presumed age of faulted deposits correlated with surficial unit Qa3 in trench T8) indicates an average recurrence interval of 50–70 k.y. during mid-Quaternary to late Quaternary time. A recurrence interval of about 35 k.y. is considered to be a minimum (two faulting events since the eruption of the Lathrop Wells volcanic center at 77±6 ka). A maximum recurrence interval of about 100 k.y. is indicated if only the two most definitive (and largest) faulting events (W, Y, table 8), are averaged over the 200-k.y. time period.

The average slip rate (dip slip) along the Solitario Canyon Fault during mid-Quaternary to late Quaternary time is estimated at 0.01 to 0.02 mm/yr, considering averages of 2.0 m of slip over 200 k.y. and 1.2 m of slip over 75 k.y. Averaging the fault slip over the past 900 k.y. (U-series age of faulted colluvium in trench SCF–T3) indicates a longer-term average slip rate of 0.002 to 0.003 mm/yr.

Possible Volcanically Related Fault Activity

The largest fissures at all four trench sites along the main Solitario Canyon Fault trace contain abundant basaltic ash. Historical-earthquake deformation shows that extensional openings begin to fill with detrital material during the first significant rainfall and invariably contain noticeable fill within weeks to months of fissuring. Angularity of the basaltic ash in the bottom of the fissure in trench T8 indicates minimal transport and, therefore, implies a local source, most likely the Lathrop Wells basaltic cone located 11 to 16 km to the south (fig. 1), dated at 77±6 ka (Heizler and others, 1999). The mixed silt, ash, and gravel in the upper fissure fill of trench T8 indicates that after the ash was largely depleted from the ground surface, the fissure filled more slowly with eolian material (silt and additional reworked ash) as debris washed in from upslope. Soil development and stratigraphic correlation support a late Pleistocene age for the fissure fill.

A cogenetic link between seismicity and volcanism was previously suggested by Swadley and others (1984), on the basis of the presence of ash in trench exposures across four different faults in the Yucca Mountain area, including trench T8 (fig. 2). The ash deposits exposed in older trenches were observed only in narrow (0.2–2 cm wide) vertical fractures, whereas the ash exposed in newer trenches across the Solitario Canyon Fault more definitively establishes a temporal association between seismicity and volcanism and indicates both more fault slip and a greater volume of ash than could be inferred from the older trenches.

Basaltic ash intermixed with silt is present in smaller fissures that both predate (trench SCF–T3, fig. 34) and postdate (north wall of trench T8, fig. 32) the conspicuous ash-filled fissures; these deposits may indicate additional faulting events of coincident surface rupture and volcanism, although reworking of ash from the large ash-filled fissures cannot be precluded. Apparent temporal clustering of faulting events in mid-Quaternary to late Quaternary time (see chap. 14), in combination with an apparent association of seismicity and

volcanism, is therefore considered as evidence that the pulse of mid-Quaternary to late Quaternary activity on the Solitario Canyon Fault is genetically linked with volcanic activity at the Lathrop Wells volcanic center (fig. 1).

Discussion

Structural and stratigraphic relations exposed in trenches across the Solitario Canyon Fault and elsewhere in the Yucca Mountain area (figs. 1, 2) are complicated by extensive carbonate overprinting and by relatively small surface offsets that are difficult to measure. Colluvial wedges (material shed from and deposited against fault scarps), which are commonly observed in trench exposures of normal faults, are generally absent in all the trenches. Three principal factors likely contribute to the paucity of colluvial wedges. First and foremost, surface displacements have occurred largely as extensional openings of steep fissures splaying from a dipping bedrock fault plane. Scarp erosion, backwasting, and deposition after such events must first fill the fissures; only after the fissures have been filled can colluvial wedges be formed. Second, surficial erosion after a faulting event is evident at all of the trench sites, as indicated by missing soil horizons and truncated fissures and stratigraphic contacts, and so colluvial wedges could be partly removed. In all the trenches, deposits of unit Qa5 (table 20) rest on these unconformities, indicating that appreciable erosion occurred during latest Pleistocene to early Holocene time. Third, small (≤0.5 m) vertical displacements are not conducive to formation of obvious colluvial wedges.

The information gained from the trenches across the Solitario Canyon Fault allows preliminary interpretations of surface rupture, but relatively large uncertainties preclude confident conclusions about fault offsets. The varying displacements do not support characteristic fault behavior (that is, recurrent faulting events with similar rupture distributions and offsets). Single-event displacements range from fracturing with no obvious displacement to possibly more than 1 m of slip associated with the largest fissuring event; most of the offsets are relatively small (no more than a few tens of centimeters). Similarly, limited geochronologic data indicate that faulting events have not occurred over regularly spaced time intervals. The apparent early Quaternary to mid-Quaternary hiatus in seismicity further indicates noncharacteristic behavior and contributes uncertainty to forecasting future fault activity. A conservative seismic-hazard assessment would be that we are still within a period of "elevated" activity and that the mid-Quaternary to late Quaternary record better reflects possible fault activity in the near future than does the entire Quaternary record.

Rather than behaving independently, some or all of the faults at Yucca Mountain may rupture together during individual seismic events or sequences (see chap. 14). Such distributive surface ruptures may be expected, on the basis of the high degree of fault interconnection and the presence of basaltic ash in fractures along multiple faults. Thus, the faults around Yucca Mountain can be considered to constitute one or more complex fault systems, rather than numerous independent faults. Uncertainties in age control and fault relations, however, likely will always limit how well seismic events can be correlated between faults. Also, it may be difficult to correlate small earthquakes on different faults, or even along individual fault traces. As evidenced by historical surface ruptures, small displacements commonly are highly discontinuous; such faulting events may cause significant offsets in some places but little or no offset in others. With regard to the Solitario Canyon Fault, one of its main splays, the Iron Ridge Fault, does not contain ash deposits or display evidence of displacement during the large penultimate event Y (table 8). Offset did occur, however, during earlier events that may coincide with earthquakes on other segments of the Solitario Canyon Fault.